Available online at www.sciencedirect.com
ScienceDirect
Applied Catalysis B: Environmental 81 (2008) 182–191
APPLIED CATALYSIS B: ENVIRONMENTAL
www.elsevier.com/locate/apcatb

Mesoporous $H_3PW_{12}O_{40}$-silica composite: Efficient and reusable solid acid catalyst for the synthesis of diphenolic acid from levulinic acid

Yihang Guo [a,b,*], Kexin Li [a], Xiaodan Yu [a], James H. Clark [b,**]

[a] School of Chemistry, Northeast Normal University, Changchun 130024, PR China
[b] Green Chemistry Centre, Department of Chemistry, University of York, Heslington, York YO10 5DD, United Kingdom

Received 23 August 2007; received in revised form 17 December 2007; accepted 29 December 2007
Available online 3 January 2008

Abstract

Mesoporous $H_3PW_{12}O_{40}$-silica composite catalysts with controllable $H_3PW_{12}O_{40}$ loadings (4.0–65.1%) were prepared by a direct sol–gel–hydrothermal technique in the presence of triblock poly(ethylene oxide)-poly(propylene oxide)-poly(ethylene oxide) copolymer. Powder X-ray diffraction (XRD) patterns and nitrogen sorption analysis indicate the formation of well-defined mesoporous materials. With $H_3PW_{12}O_{40}$ loading lower than 20%, the materials exhibit larger BET surface area (604.5–753.0 $m^2\ g^{-1}$), larger and well-distributed pore size (6.1–8.6 nm), larger pore volume (0.75–1.2 $cm^3\ g^{-1}$), and highly dispersed Keggin unit throughout the materials. Raman scattering spectroscopy studies confirm that the primary Keggin structure remained intact after formation of the composites. As a novel kind of reusable solid acid catalyst, as-prepared $H_3PW_{12}O_{40}$-silica composite was applied for the synthesis of diphenolic acid (DPA) from biomass platform molecule, levulinic acid (LA), under solvent-free condition, and remarkably high catalytic activity and stability were observed.

Keywords: Diphenolic acid; Biomass platform molecule; Levulinic acid; Mesoporous materials; Heteropoly acids; Sol−gel

1. Introduction

Diphenolic acid (DPA) is a structural analog of bisphenol A (BPA). It is prepared by the condensation reaction of phenol with levulinic acid (LA) in the presence of Brönsted acid. It can be substituted for BPA, the primary raw material of epoxy resin [1–3]. The lower cost of BPA has reduced the market for DPA, however, the rapid escalating cost of petrochemicals are accelerating the shift towards chemical products derived from renewable, biological feedstocks. LA is one of the top biomass platform molecules. It can be made by the treatment of 6-carbon sugar carbohydrates from starch or lingocellulosics with acid. It has frequently been suggested as the starting material for a wide number of compounds [4]. The development of DPA as a BPA replacement and the investigation of the properties of the resulting polymers will provide new sustainable opportunities for the chemical industry. Traditional catalysts for the synthesis of DPA are strong Brönsted mineral acids (HCl or H_2SO_4) [2]. In recent years, environmental and economic considerations have encouraged the redesign of commercially important processes so that the use of harmful substances and the generation of toxic waste are avoided. Heterogeneous catalysis can play a key role in the development of environmentally benign processes for the production of chemicals and especially where it replaces liquid acid catalysts [5]. Zeolites have attracted considerable attention as solid acids, but they present severe limitations when large reactant and/or product molecules are involved. Heterogeneous acid catalysis using heteropoly acids (HPAs) has potential economic and green benefits. The majority of the reported catalytic applications use the most common Keggin type HPAs [6]. While HPAs provide strong Brönsted acidity, HPAs in the bulk form are of poor efficiency due to low surface area and a consequential limited number of available acid sites for catalytic reactions [7,8]. HPAs are readily soluble in many

* Corresponding author at: School of Chemistry, Northeast Normal University, Changchun 130024, PR China. Tel.: +86 431 85098705; fax: +86 431 85098705.
** Corresponding author. Tel.: +44 1904 432559; fax: +44 1904 434550.
E-mail addresses: guoyh@nenu.edu.cn (Y. Guo), jhc1@york.ac.uk (J.H. Clark).

0926-3373/$ – see front matter © 2008 Elsevier B.V. All rights reserved.
doi:10.1016/j.apcatb.2007.12.020

solvents, which results in a difficult separation and recovery from the reaction mixture. Therefore, methods for the preparation of water-tolerant solid HPAs have been developed [9–15]. Two common routes, a post-synthesis grafting method and a direct co-condensation sol–gel method, have been used for this purpose. The conventional post-synthesis grafting method suffers from several drawbacks including poor control over HPA loading, HPA leaching, and the loss of homogeneity due to minor changes in the structure. All of these lead to reduced activity of the immobilized HPAs. The reported silica-included Keggin units, $H_3PW_{12}O_{40}/SiO_2$ and $H_4SiW_{12}O_{40}/SiO_2$, have been prepared by a direct co-condensation sol–gel method without adding a structure-directing agent. These materials are microporous with a pore size of *ca*. 0.6 nm and BET surface area of 400–800 $m^2\ g^{-1}$ [16,17]. Most importantly, leaching of the immobilized Keggin units during the catalytic process was reduced. However, these materials suffer from similar diffusional problems to zeolites. Therefore, the development of routes to solid HPAs with larger pore sizes and higher surface areas is necessary to enable a complete realization of the potential of HPA catalysis.

A combination of extremely large surface areas and flexible pore sizes makes surfactant-templated ordered mesostructured materials interesting supports for developing novel water-tolerant and catalytically useful HPA materials of the various known ordered mesostructured materials. Silicate-based periodic mesoporous silica like MCM-41, MCM-48, and SBA-15 are known to be excellent supports for the dispersion of HPAs [18,19]. By considering the structural properties of $H_3PW_{12}O_{40}$ we have chosen SBA-15 silica as the support for the Keggin unit in this study. Mesostructured silica-supported $H_3PW_{12}O_{40}$ materials with controllable $H_3PW_{12}O_{40}$ loadings and unique porosities were prepared by simultaneous hydrolysis and condensation of tetraethoxysilane (TEOS) with $H_3PW_{12}O_{40}$ in the presence of template surfactant, Pluronic P123 ($EO_{20}PO_{70}EO_{20}$; EO, ethylene oxide; PO, propylene oxide) followed by subsequent steps of hydrothermal treatment and template removal. Several factors have been considered in the design of the preparation route: (i) need to avoid decomposition of the Keggin structure; (ii) minimize loss of the $H_3PW_{12}O_{40}$; (iii) disperse $H_3PW_{12}O_{40}$ unit throughout the co-condensation materials. The structural and textural properties of as-prepared $H_3PW_{12}O_{40}$/silica have been characterized by Raman scattering spectroscopy, powder X-ray diffraction (XRD), nitrogen porosimetry, and transmission electron microscopy (TEM). These materials were subsequently utilized as solid acid catalysts in the condensation reaction of phenol with LA to produce DPA. It was found that as-prepared materials show remarkably high catalytic activity and stability in this reaction system. These materials could serve as novel solid acid catalysts in many acid-catalyzed reactions.

2. Experimental

TEOS (98.0%), 12-tungstophosphoric acid (99.9%), P123 (MW 5800), and LA (99.9%) were purchased from Aldrich. DPA (99%) was purchased from BASF. All reagents were used as purchased without further purification.

2.1. Preparation of $H_3PW_{12}O_{40}$/silica composites

In a typical preparation of $H_3PW_{12}O_{40}$/silica, P123 (1.80 g, 3.1×10^{-4} mol) was dissolved in ethanol (4.74 g, 0.10 mol) at room temperature, and TEOS (3.26 g, 0.016 mol) was diluted with ethanol (1.58 g, 0.033 mol). In another container, the desired amount of $H_3PW_{12}O_{40}$ was dissolved with water (2.5 g, 0.12 mol). The amount of $H_3PW_{12}O_{40}$ added was in the range of 0.1–0.6 g or 3.33×10^{-5} to 2.00×10^{-4} mol to ensure 10–60% $H_3PW_{12}O_{40}$ loadings in the products. The above TEOS/EtOH solution and aqueous $H_3PW_{12}O_{40}$ solution was added dropwise into the P123/EtOH solution, respectively, at room temperature. Stirring was used throughout the process. The acidity of the mixture was controlled at pH 1.2 ± 0.2 by HCl (12 mol L^{-1}). After homogenizing the mixture for 3 h, the clear sol was subjected to hydrothermal treatment at 110 °C for 48 h at a heating rate of 2 °C/min. The transparent hydrogel obtained was dehydrated slowly at 45 °C in a vacuum for 24–48 h until complete gel particulate was formed. The dried gel was calcined at 80, 100, and 120 °C for 2 h, successively, in vacuum. The product was washed with dilute HCl (0.5 mol L^{-1}) at 60 °C for three times. And then half of the dried powder was refluxed in boiling absolute ethanol (30 mL) containing 1 mL of HCl (12 mol L^{-1}) for 3 h, and the procedure was repeated three times. The other half of the dried powder was calcined at 420 °C at a heating rate of 2 °C/min. The final products are denoted as $H_3PW_{12}O_{40}/SiO_2$-C/E−x, where C/E refers to the catalyst obtained by calcination/extraction for P123 removal, and x is the $H_3PW_{12}O_{40}$ loading (wt%) in the composite. FT-IR results showed that P123 was almost removed after the procedure of extraction or calcination. For comparative purposes, another kind of silica-based $H_3PW_{12}O_{40}$ composite was also prepared in the absence of the surfactant P123 according to the above procedure, and it is denoted as $H_3PW_{12}O_{40}/SiO_2$−x without P123.

2.2. Characterization

Loading of $H_3PW_{12}O_{40}$ was determined on a Leeman Prodigy Spec inductively coupled plasma atomic emission spectrometer (ICP-AES). Nitrogen porosimetry was performed on a Micromeritics ASAP 2010 instrument. Surface areas were calculated using the BET equation. Pore size distributions were estimated from BJH desorption determination (the samples were outgassed under vacuum at 120 °C overnight). Low- and wide-angle XRD patterns of the composites were obtained on a D/max-2200 VPC diffractometer using Cu Kα radiation. Raman scattering spectra were recorded on a Jobin-Yvon HR 800 instrument with an Ar^+ laser source of 488 nm wavelength in a macroscopic configuration. TEM images were recorded on a JEOL JEM-2010 transmission electron microscope at an accelerating voltage of 200 kV.

2.3. Catalytic experiments

The solid catalysts were calcined at 120 °C under vacuum for 3 h prior to the catalytic experiments. The condensation of

LA with phenol to produce DPA was carried out in a sealed glass vessel at 100 °C for 8 h. A typical experiment included a mixture of 1.32 g (0.0136 mol) of phenol, 0.4 g (0.0034 mol) of LA with 0.05 g of the catalyst. After the reaction, a measured amount of acetonitrile was added, the suspension was centrifuged and the resulting solution was further diluted with acetonitrile and then analyzed on an Applied Biosystem liquid chromatography (C_8 column)-Q-Trap triple quadrupole mass spectrometer equipped with electrospray ionization source. The instrument was interfaced to a computer running Applied Biosystems Analyst version 1.4 software, which is capable of recording ions up to *m/z* 1700. The concentrations of LA, DPA (*p,p'*) and DPA (*o,p'*) were determined simultaneously with the retention time of 1.31, 1.60, and 1.86 min, respectively.

3. Results and discussion

3.1. Catalyst preparation

The efficient immobilization of a catalytically active component within a solid support is fundamentally important in the design of heterogeneous catalysts for organic reactions. Catalytic activity and stability on reaction work-up are important attributes for a useful solid catalyst. For this purpose, the sol–gel process is a powerful tool [20]. Herein, the preparation of mesostructured $H_3PW_{12}O_{40}/SiO_2$ materials was performed by a direct co-condensation sol–gel technique combined with hydrothermal treatment. During the $H_3PW_{12}O_{40}/SiO_2$ design and preparation process, the following two factors have been considered. Firstly, formation of mesostructured $H_3PW_{12}O_{40}/SiO_2$ materials should not destroy the primary Keggin structure. $H_3PW_{12}O_{40}$ begins to decompose at pH higher than 1.5 and loses all acidic protons at 465 °C [21,22]. Therefore, the preparation should be performed under strong acid conditions. On the other hand, the interaction between the surfactant and inorganic wall should not be too strong, so that the mesostructure assembly can take place and the surfactant can be easily removed without damage to the integrity of the channel walls and Keggin structure. For this purpose, SBA-15 rather than the MCM series of molecular sieves is preferred as the support to disperse the Keggin unit. The former uses the nonionic amphiphilic block copolymer $EO_{20}PO_{20}EO_{20}$ as a structure-directing agent. Supramolecular rather than chemical interactions occur between $EO_{20}PO_{20}EO_{20}$ and the inorganic wall [23]. Thus $EO_{20}PO_{20}EO_{20}$ can be easily removed by ethanol extraction. For the latter, ionic surfactant cetyltrimethylammonium bromide (CTAB) is used as the structure-directing agent, and strong electrostatic interactions and/or covalent bonding may happen during the mesostructure assembly process. Therefore calcination at relatively high temperature (500–600 °C) is necessary for CTAB removal. Furthermore, mesostructure assembly for the MCM series of molecular sieves occurs under basic condition, which is also unsuitable for the co-condensation preparation of the supported $H_3PW_{12}O_{40}$. Secondly, loss of the $H_3PW_{12}O_{40}$ should be minimized during the process of template removal by boiling ethanol. Extraction is a better method to lead to mesostructured $H_3PW_{12}O_{40}/SiO_2$ materials. However, as $H_3PW_{12}O_{40}$ has a high solubility in ethanol the method may result in loss of most of the immobilized $H_3PW_{12}O_{40}$. In order to avoid loss of $H_3PW_{12}O_{40}$, the following steps were used to ensure strong interactions between the Keggin unit and the silica matrix: (i) simultaneous hydrolysis and condensation of TEOS with $H_3PW_{12}O_{40}$ in the presence of $EO_{20}PO_{20}EO_{20}$ under strong acid condition, and the resulting clear sol of $H_3PW_{12}O_{40}/Si(OEt)_{4-x}(OH_2^+)_x{-}EO_{20}PO_{20}EO_{20}$ was subjected to hydrothermal treatment at 110 °C for 48 h at a heating ramp of 2 °C/min; (ii) the resulting homogeneous hydrogel was dehydrated slowly at 45 °C; (iii) calcination of the dried gel particulate was carried out at 80, 100, and 120 °C, successively. After the above three steps, the silica framework was retained, and the interactions between the Keggin unit and silica matrix were strengthened. Therefore $H_3PW_{12}O_{40}$ still maintained relatively high loadings in as-prepared composites after acidified water washing and boiling ethanol extraction (see Table 1).

3.2. Compositional and structural information

The determined $H_3PW_{12}O_{40}$ loadings are as expected (Table 1), implying that the preparation method employed can effectively inhibit the loss of the Keggin unit during the

Table 1
Structural and textural information of as-prepared silica supports and $H_3PW_{12}O_{40}/SiO_2$ materials

Sample	S_{BET} ($m^2\ g^{-1}$)	D_P[a] (nm)	V_p[b] ($cm^3\ g^{-1}$)	*d* spacing (Å)
$H_3PW_{12}O_{40}/SiO_2$-E-4.0	691.6	7.1	1.20	92.91
$H_3PW_{12}O_{40}/SiO_2$-E-7.5	693.2	7.2	1.12	92.91
$H_3PW_{12}O_{40}/SiO_2$-E-14.8	683.0	7.6	0.95	95.94
$H_3PW_{12}O_{40}/SiO_2$-E-17.5	630.4	8.6	1.16	98.08
$H_3PW_{12}O_{40}/SiO_2$-C-7.5	753.0	6.0	1.10	92.91
$H_3PW_{12}O_{40}/SiO_2$-C-10.9	727.8	6.3	0.92	97.00
$H_3PW_{12}O_4$/SBA-15-C-11.3	713.2	6.4	0.85	91.95
$H_3PW_{12}O_{40}/SiO_2$-C-15.7	604.5	6.6	0.75	97.00
$H_3PW_{12}O_{40}/SiO_2$-C-58.2	375.1	6.8	0.34	–
$H_3PW_{12}O_{40}/SiO_2$-C-65.1	360.6	7.2	0.25	–
$H_3PW_{12}O_{40}/SiO_2$-15.4 without P123	317.6	1.2	0.34	–
SiO_2-E	858.2	5.2	0.71	89.16
SiO_2-C	750.1	5.3	0.51	91.95

[a] Pore diameters are estimated from BJH desorption determination.
[b] Pore volume is estimated from the pore volume determined using the adsorption branch of the N_2 isotherm curve at the $P/P_0 = 0.99$ single point.

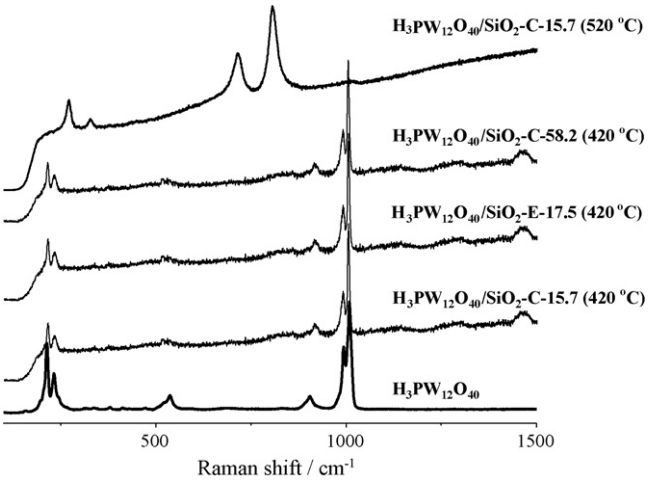

Fig. 1. Raman scattering spectra of pure $H_3PW_{12}O_{40}$ and $H_3PW_{12}O_{40}/SiO_2$ composites.

template extraction process. Structural integrity of the Keggin unit is confirmed by Raman scattering studies (Fig. 1). Raman scattering spectroscopy is an effective method to study the structure of the supported HPA because it is extremely sensitive to the Keggin unit, and the support has no significant interference on the Raman signals originating from the Keggin unit [24]. The Raman scattering peaks found in the range of 1100–900 cm^{-1} are assigned to the Keggin unit, which correspond to stretching vibrations of P–O bonds of the PO_4 sites (1009.5 cm^{-1}), W=O bonds (993.9 cm^{-1}) and W–O–W bonds (912.4 cm^{-1}) of the Keggin unit. After formation of the extracted $H_3PW_{12}O_{40}/SiO_2$ material, these three peaks are also observed with some shifts of the peak positions (Table 2). Similar results are observed for the calcined materials with a calcination temperature of 420 °C. However, for the material with a calcination temperature of 520 °C it is difficult to found the Raman scattering peak corresponding to the stretching vibrations of P–O bonds, and at the same time, a significant redshift is observed for the other two peaks corresponding to the stretching vibrations of the W=O and W–O–W bonds. The above results indicate that the primary Keggin structure remained intact after the formation of the mesostructured silica-based composites by extraction or calcination at a relatively low temperature (420 °C) for P123 removal. The shifts of the peak positions are due to strong interactions between the Keggin unit and the silica support, which interfere with the symmetry of the Keggin unit. However, calcination at a relatively high temperature (520 °C) for P123 removal resulted in partial decomposition of the Keggin structure.

Table 2
Characteristic Raman shifts (cm^{-1}) of the $H_3PW_{12}O_{40}$ in the $H_3PW_{12}O_{40}/SiO_2$ composites

Sample	W–O–W	W=O	P–O
$H_3PW_{12}O_4$	912.4	993.9	1009.5
$H_3PW_{12}O_{40}/SiO_2$-E-17.5	916.8	991.3	1005.0
$H_3PW_{12}O_{40}/SiO_2$-C-15.7[a]	917.0	991.3	1005.6
$H_3PW_{12}O_{40}/SiO_2$-C-58.2[a]	918.3	990.2	1005.9
$H_3PW_{12}O_{40}/SiO_2$-C-15.7[b]	714.5	806.8	1008.0

[a] Template removal temperature was 420 °C.
[b] Template removal temperature was 520 °C.

3.3. Mesostructure, morphology, and porosity

The low-angle XRD patterns of the surfactant-free silica-based $H_3PW_{12}O_{40}$ materials with $H_3PW_{12}O_{40}$ loading lower than 20% demonstrate main characteristic reflection in the range of 98.08–91.95 Å (*d* spacings) and equivocal reflection in the range of 67.90–44.14 Å. (Fig. 2 and Table 1). And difference of *d* value among the extracted and calcined $H_3PW_{12}O_{40}/SiO_2$ materials is hardly noticeable. The result indicates that the mesostructure of the composites is poor ordered due to the introduction of the Keggin unit. Further increasing $H_3PW_{12}O_{40}$ loadings to 58.2 and 65.1%, respectively, we failed to detect the above reflections, implying the mesostructure of $H_3PW_{12}O_{40}/SiO_2$-C-58.2 and $H_3PW_{12}O_{40}/SiO_2$-C-65.1 is completely disordered.

The wide-angle XRD patterns of the $H_3PW_{12}O_{40}/SiO_2$ materials are shown in Fig. 3. The results can be used to study the dispersion of the Keggin unit throughout the composites. The composites with $H_3PW_{12}O_{40}$ loadings lower than 17.5% exhibit a broad diffraction peak (2θ = 15–30°), which can typically be attributed to amorphous silica. No diffraction peaks corresponding to the starting $H_3PW_{12}O_{40}$ are found. However, $H_3PW_{12}O_{40}$ diffraction peaks are found in the $H_3PW_{12}O_{40}/SiO_2$-C-58.2 composite at 23.2 (442), 28.6 (642), 33.3 (555), and 41.6° (953), respectively. The $H_3PW_{12}O_{40}/SiO_2$-C-65.1 composite calcined at 520 °C shows that the decomposition and aggregation of the Keggin unit happened simultaneously. The above results demonstrate that the Keggin units with lower loadings (20%) in the composites are homogeneously dispersed

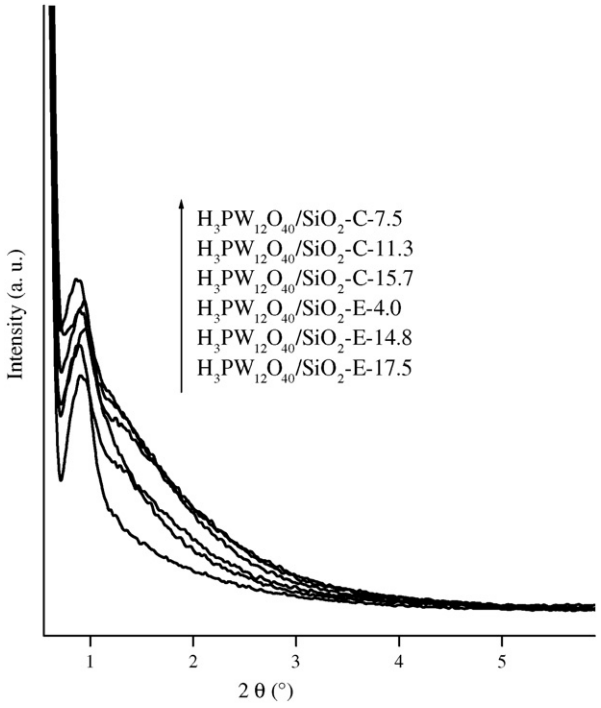

Fig. 2. Low-angle XRD patterns of the $H_3PW_{12}O_{40}/SiO_2$ composites.

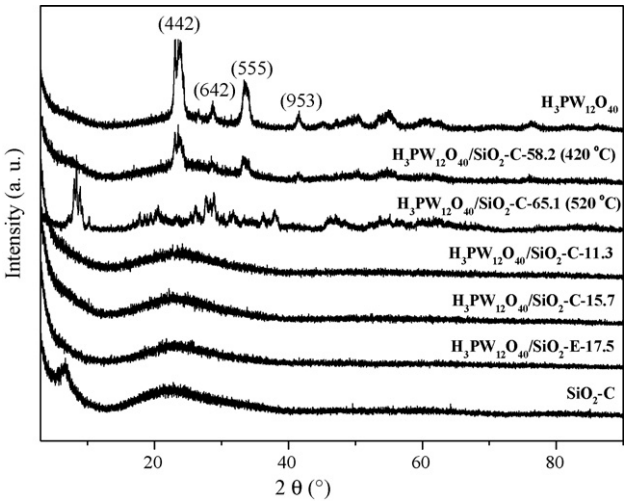

Fig. 3. Wide-angle XRD patterns of the $H_3PW_{12}O_{40}/SiO_2$ composites.

throughout the composites, but higher $H_3PW_{12}O_{40}$ loadings lead to their uneven dispersion or aggregation across the composites.

The morphology of the composite was studied by TEM, and the representative results are shown in Fig. 4. These images reveal that $H_3PW_{12}O_{40}/SiO_2$-E-14.8 composite is three-dimensionally interconnected pore-network structure with poor ordered but high porosity. Formation of this morphology is due to the current preparation route, which is different from the standard method for the preparation of SBA-15 silica [22]. In addition, introduction of the large Keggin unit (size of 1.0 nm) into silica network may interfere with the observation of the porous structure of the composites. Therefore, the pore sizes of the composites were obtained by N_2 porosimetry results.

All of the isotherms (Fig. 5A and C) for the tested materials are type IV. This shows that the capillary condensation occurs at higher relative pressures ($p/p_0 = 0.45$–0.85) regardless of the methods used for the template removal (extraction/calcination). This is consistent with mesoporous materials tailored by nonionic templates [23]. With the exception of the materials $H_3PW_{12}O_{40}/SiO_2$-C-58.2 and $H_3PW_{12}O_{40}/SiO_2$-C-65.1, all other eight tested samples showed very high pore volume and large BET surface areas even after introduction of the Keggin unit into the silica matrix (Table 1). Also, their pore sizes are larger than those of the corresponding silica supports (SiO_2-E and SiO_2-C). In addition, although the BET surface areas have decreased somewhat after incorporation of the Keggin units on silica support, their pore volume have increased. The difference in BET surface area and pore volume between the calcined samples and extracted ones are insignificant. The narrow pore size distributions (Fig. 5B and D) of the $H_3PW_{12}O_{40}/SiO_2$ materials with $H_3PW_{12}O_{40}$ loadings lower than 20% imply that the composites exhibit uniform pore sizes, and the Keggin units are homogeneously distributed across the sol–gel co-condensed materials. Interestingly, the onset of the capillary condensation step occurs at increasing relative pressures with increasing $H_3PW_{12}O_{40}$ loading from 0 to 17.5%. This implies that the average pore size increases with $H_3PW_{12}O_{40}$ loading increasing. The conclusion is consistent with the pore diameters calculated with the BJH method on the desorption branch of the N_2 sorption isotherms (Table 1). With increasing $H_3PW_{12}O_{40}$ loading to 58.2 and 65.1%, respectively, the resulting BET surface area and pore volume decrease obviously, suggesting that the materials are increasingly disordered with higher $H_3PW_{12}O_{40}$ loadings. The result is consistent with the low-angle XRD determination, further confirming partial blocking of the pore openings after a large amount of the Keggin units were introduced.

Repeat preparations were performed on several of the materials ($H_3PW_{12}O_{40}/SiO_2$-15-E-14.8 and $H_3PW_{12}O_{40}/SiO_2$-E-17.5; $H_3PW_{12}O_{40}/SiO_2$-C-10.9 and $H_3PW_{12}O_{40}/SiO_2$-C-11.3; $H_3PW_{12}O_{40}/SiO_2$-C-58.2 and $H_3PW_{12}O_{40}/SiO_2$-C-65.1) to validate the reproducibility of the textural properties. All samples tested gave satisfactory results (Table 1).

On the basis of the above results and Zhao's work [22], we postulate that the assembly of the mesoporous $H_3PW_{12}O_{40}/SiO_2$ materials organized by triblock copolymer species in acid media occurs through the following steps. First, TEOS is hydrolyzed in the presence of $H_3PW_{12}O_{40}$ and $EO_{20}PO_{70}EO_{20}$

$$H_3PW_{12}O_{40} + Si(OEt)_4 + nH_3O^+ \xrightarrow[pH\,1.0\pm2.0]{\text{hydrolysis}} H_3PW_{12}O_{40}/Si(OEt)_{4-n}(OH_2^+)_n + n\text{EtOH} \quad (1)$$

The interaction between the Keggin unit and silica species is chemical, and the interacting species may be formed by proton

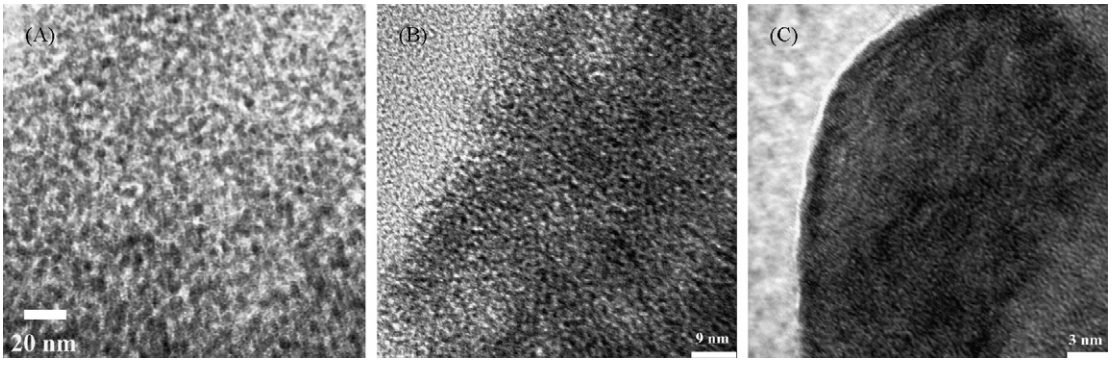

Fig. 4. TEM images of $H_3PW_{12}O_{40}/SiO_2$-E-14.8 at different magnifications.

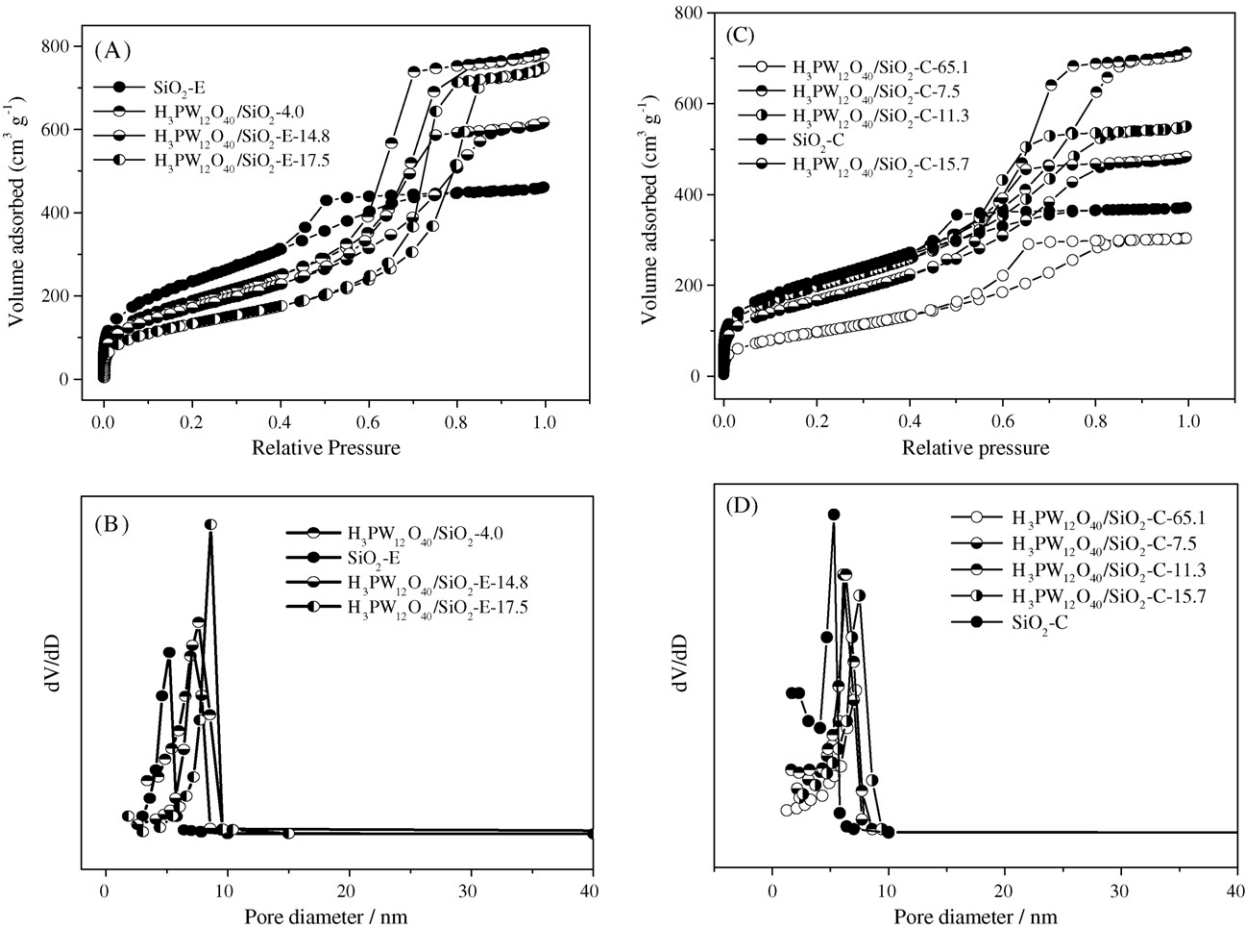

Fig. 5. Nitrogen adsorption–desorption isotherms (A and C) and pore size distribution profiles (B and D) according to BJH desorption d*V*/d*D* pore volume of $H_3PW_{12}O_{40}/SiO_2$ materials.

transfer as shown in the following equation [14]:

$$H_3PW_{12}O_{40} + \equiv Si{-}OH \rightarrow (\equiv Si{-}OH_2)^+(H_2PW_{12}O_{40})^- \quad (2)$$

The EO moieties of $EO_{20}PO_{70}EO_{20}$ in strong acid media associate with hydronium ions

$$REO_m + yHCL \xrightarrow{H_2O} REO_{m\text{-}y}[(EO)\cdot H_3O^+]_y \cdots yC^- \quad (3)$$

where R is the poly(propylene oxide). The charge-associated EO units and the cationic silica species are assembled together by a hydrogen bonding and/or electrostatic interactions and form $REO_{m-y}[(EO)\cdot H_3O^+]_y \cdots yCl^- \cdots H_3PW_{12}O_{40}/Si(OEt)_{4-n}(OH_2^+)_n$. Further condensation of the silica species and organization of the surfactant and inorganic species result in solidifying the inorganic network and forcing interactions between the Keggin unit and the silica matrix. These steps were achieved by hydrothermal treatment of the sol of $H_3PW_{12}O_{40}/Si(OEt)_{4-n}(OH_2^+)_n\text{-}EO_{20}PO_{70}EO_{20}$ species, which was dehydrated slowly at low temperature, followed by gradual calcination of the resulting gel particulates at 80, 100, and 120 °C. After removal of the template by ethanol extraction or calcination mesoporous $H_3PW_{12}O_{40}/SiO_2$ material is formed. On the basis of the results of N_2 sorption determinations we infer that $H_3PW_{12}O_{40}/SiO_2$ species formed *via* interaction of the protons from the Keggin units and hydroxyl groups of silanol from the silica are located inside the pores, resulting in larger pore sizes of the products than those of the parent silica support. In the absence of the $EO_{20}PO_{70}EO_{20}$, the resulting $H_3PW_{12}O_{40}/SiO_2$ composite with $H_3PW_{12}O_{40}$ loading of 15.4% exhibits obvious disordered microporosity with a pore size of 1.2 nm and BET surface area of 317.6 $m^2\ g^{-1}$ (Table 1). This suggests that nonionic surfactant $EO_{20}PO_{70}EO_{20}$ does play an important role for the construction of well-defined mesostructure of $H_3PW_{12}O_{40}/SiO_2$ materials with larger pore sizes and surface areas.

3.4. Catalytic condensation of phenol with LA to produce DPA

Condensation of phenol with LA to produce DPA is a typical Brönsted acid-catalyzed reaction, and its reaction mechanism is shown in Scheme 1. The acid catalytic activity of as-prepared $H_3PW_{12}O_{40}/SiO_2$ is evaluated by this reaction. For comparison, HCl, $H_3PW_{12}O_{40}$, $H_3PW_{12}O_{40}/SiO_2$-15.4 without P123, and the silica support were also tested for this reaction, and the results are summarized in Table 3 and Figs. 6–9. Under solvent-free and excess phenol (4 mol/mol LA) conditions, all acid catalysts tested are quite efficient for this reaction although the silica support itself is inert. Under the reaction conditions

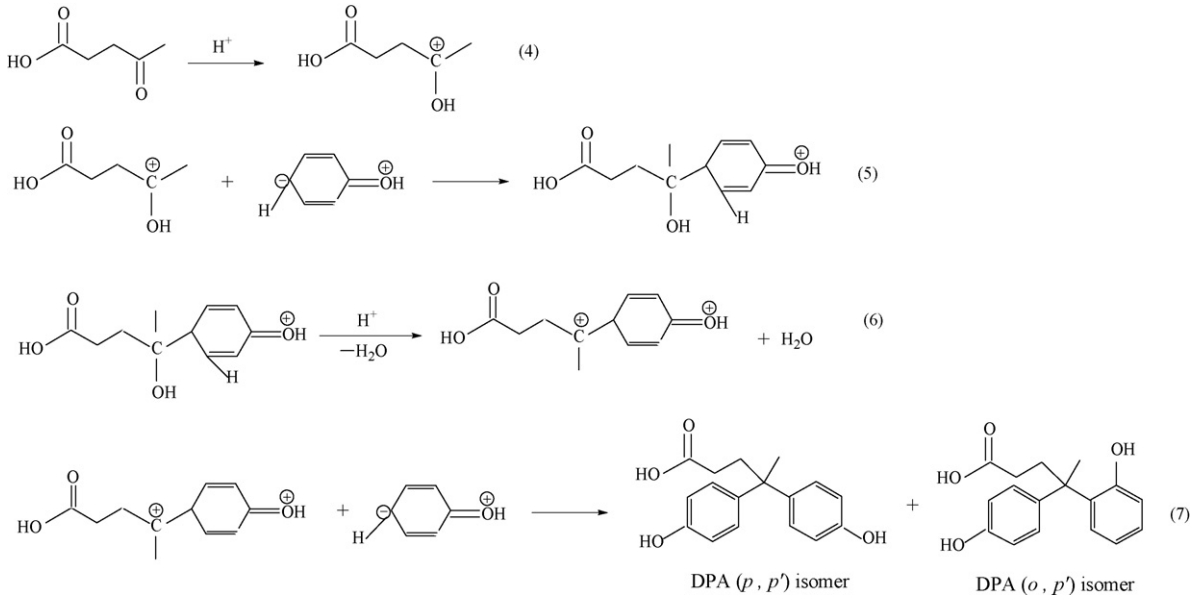

Scheme 1. Reaction mechanism for the acid-catalyzed condensation of phenol with LA to produce DPA.

applied, the two structural isomers of DPA were formed in all cases (see Scheme 1). The TOFs listed in Table 3 represents the total molar quantity of the two isomers divided by total molar quantity of active site (HCl or $H_3PW_{12}O_{40}$).

The influence of reaction parameters including mass of the catalyst, reaction temperature, and molar ratio of phenol to LA on the yield of DPA (total quantity of the two DPA isomers) and/or selectivity were studied. The yield of DPA increased with increasing catalyst quantity ($H_3PW_{12}O_{40}/SiO_2$-C-15.7) up to a point but thereafter a further increase in the mass of catalyst had little effect. In our current catalytic system, mass of the catalyst used is 50 mg for all catalytic experiments. The reaction was carried out at 80, 100, and 120 °C, respectively, to evaluate the influence of reaction temperature (Fig. 7). As expected, the DPA yield increased with increasing the reaction temperature although the selectivity to *p*,*p*'-DPA decreased somewhat (Table 4).

The molar ratio of phenol to LA is one of the important parameters that affect the yield of DPA. From the result shown in Fig. 8A it can be seen that increasing the phenol to LA molar ratio from 2:1 to 5:1 led to DPA yield increasing from 31.8 to 37.5% after the reaction proceeds for 6 h by using $H_3PW_{12}O_{40}/SiO_2$-E-14.8 catalyst. Under the same condition, the selectivity of *p*,*p*'-DPA to *o*,*p*'-DPA increased from 2.0 to 2.9 (Fig. 8B). To further study the influence of the molar ratio of phenol to LA on the isomer ratios, other heterogeneous acid catalysts including $C_{2.5}H_{0.5}PW_{12}O_{40}$ [25], $H_3PW_{12}O_{40}/Ta_2O_5$-12.8 [26], SO_3H/SBA-15 [27], and MCM-49 (calcined at 500 °C before catalytic test) were also examined (Fig. 8B). The interesting result shows that

Table 3
Catalytic properties of as-prepared $H_3PW_{12}O_{40}/SiO_2$ and reference materials for the condensation of phenol with LA to produce DPA[a]

Entry	Catalyst	LA conversion (%)	TOF[b]	*p*,*p*'/*o*,*p*' (molar ratio)
1	$H_3PW_{12}O_{40}/SiO_2$-E-4.0	23.6	6.9	3.6
2	$H_3PW_{12}O_{40}/SiO_2$-E-7.5	31.3	8.6	2.8
3	$H_3PW_{12}O_{40}/SiO_2$-E-14.8	74.8	46.4	3.0
4	$H_3PW_{12}O_{40}/SiO_2$-E-17.5	80.1	51.0	2.8
5	$H_3PW_{12}O_{40}/SiO_2$-C-7.5	19.2	3.5	2.1
6	$H_3PW_{12}O_{40}/SiO_2$-C-10.9	66.2	33.1	3.1
7	$H_3PW_{12}O_{40}/SiO_2$-C-11.3	72.3	48.5	3.6
8	$H_3PW_{12}O_{40}/SiO_2$-C-15.7	80.3	53.9	2.9
9	$H_3PW_{12}O_{40}/SiO_2$-C-58.2	43.6	15.8	2.8
10	$H_3PW_{12}O_{40}/SiO_2$-C-65.1	39.4	13.8	2.6
11	$H_3PW_{12}O_{40}/SiO_2$-15.4 without P123	7.6	0.65	2.8
12	$H_3PW_{12}O_{40}$	60.1	1.04	2.9
13	HCl	65.4	0.73	2.2
14	SiO_2-E	0	0	–
15	SiO_2-C	0	0	–

[a] 3.4 mmol LA, 13.6 mmol phenol, 50 mg catalyst, 100 °C, 8 h.
[b] TOF is based on mol of DPA/mol of active site.

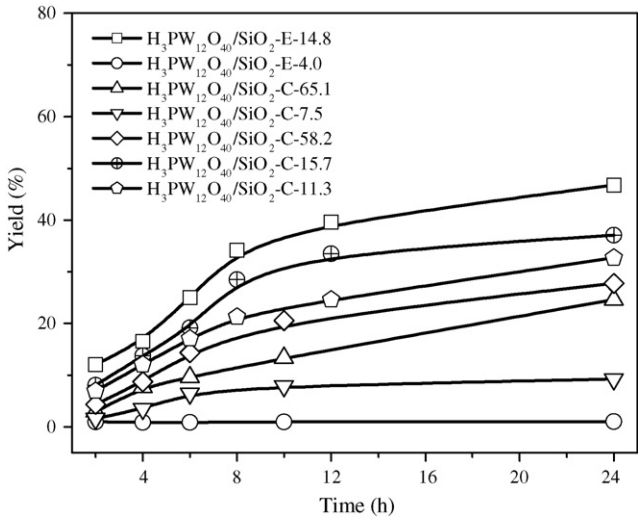

Fig. 6. Catalytic activity of synthesis of DPA from LA catalyzed by the $H_3PW_{12}O_{40}/SiO_2$ materials with different $H_3PW_{12}O_{40}$ loadings and template removal methods. 3.4 mmol LA; 13.6 mmol phenol; 50 mg catalyst; 100 °C.

different solid acids resulted in different *p,p'*-DPA to *o,p'*-DPA ratios. In the cases of $C_{2.5}H_{0.5}PW_{12}O_{40}$ and SO_3H/SBA-15, the selectivity increased with the molar ratio increasing. This result is similar to that of as-prepared $H_3PW_{12}O_{40}/SiO_2$-E-14.8. As for the MCM-49, the opposite result was obtained, and increasing the molar ratio led to decreased *p,p'*-DPA to *o,p'*-DPA ratio. For our previous reported microporous $H_3PW_{12}O_{40}/Ta_2O_5$-12.8 composite prepared by a sol–gel method without structure-directing reagent, the *p,p'*-DPA to *o,p'*-DPA ratio maintained constant regardless of the molar ratios. The above different selectivity for various solid acids may be owing to their different surface physicochemical properties.

The conversion of LA is higher using homogeneous HCl or $H_3PW_{12}O_{40}$ as the catalyst compared to our materials. However, decreased TOF is obtained compared with as-prepared $H_3PW_{12}O_{40}/SiO_2$ (entries 12 and 13 in Table 3). The

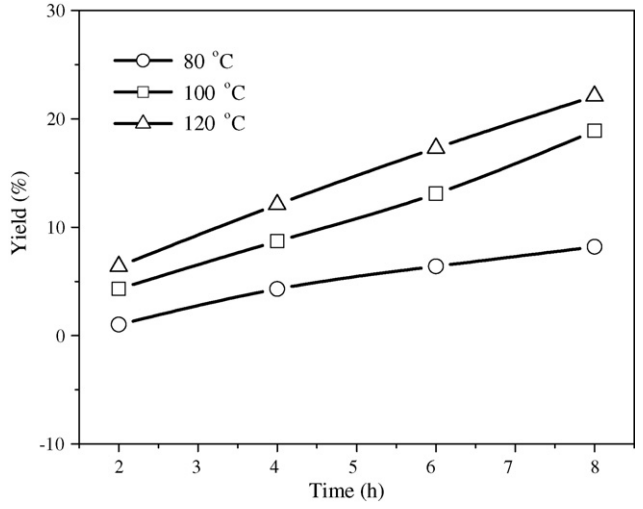

Fig. 7. Effect of reaction temperature on the yield of DPA. $H_3PW_{12}O_{40}/SiO_2$-14.8 was used (50 mg). 3.4 mmol LA; 13.6 mmol phenol; 100 °C.

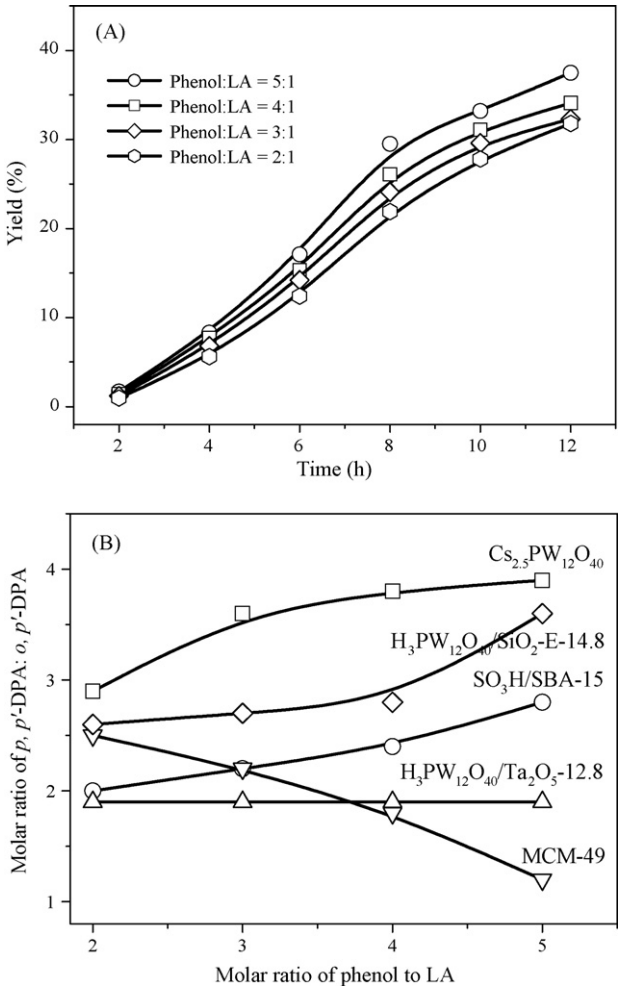

Fig. 8. Effect of molar ratios of phenol to LA on the yield of DPA ((A) $H_3PW_{12}O_{40}/SiO_2$-E-14.8 was used) and selectivity of *p,p'*-DPA to *o,p'*-DPA (B). 50 mg catalyst; 100 °C, 6 h.

ratio of *p,p'*-DPA to *o,p'*-DPA is around three regardless of the $H_3PW_{12}O_{40}$ loadings. However, significant difference in the catalytic activities (both conversion and TOF) is observed for the $H_3PW_{12}O_{40}/SiO_2$ materials with different $H_3PW_{12}O_{40}$ loadings (entries 1–10 in Table 3). Both LA conversion and TOF increase significantly with increasing $H_3PW_{12}O_{40}$ loadings from 4.0 to 17.5% for both the extracted and calcined $H_3PW_{12}O_{40}/SiO_2$ samples (entries 1–8 in Table 3). However, with an increase of the $H_3PW_{12}O_{40}$ loading to 58.2 and 65.1%, respectively, the activity decreased (entries 9–10 in Table 3). In addition, the activity of $H_3PW_{12}O_{40}$/silica-15.4 without P123 is much lower than the mesoporous $H_3PW_{12}O_{40}/SiO_2$ (entry 11 in Table 3). With the same $H_3PW_{12}O_{40}$ loading (7.5%) but different surfactant removal methods, the catalytic performance of the catalyst is different. That is, the catalytic activity of the extracted sample ($H_3PW_{12}O_{40}/SiO_2$-E-7.5, entry 2) is higher than the calcined sample ($H_3PW_{12}O_{40}/SiO_2$-C-7.5, entry 5).

Determining the cause of the higher activity for the $H_3PW_{12}O_{40}/SiO_2$ materials requires understanding of the relative importance of their active site concentrations (BET surface areas, pore volume, and $H_3PW_{12}O_{40}$ loadings) and the bulk structure of the materials [23]. Generally, catalytic activity

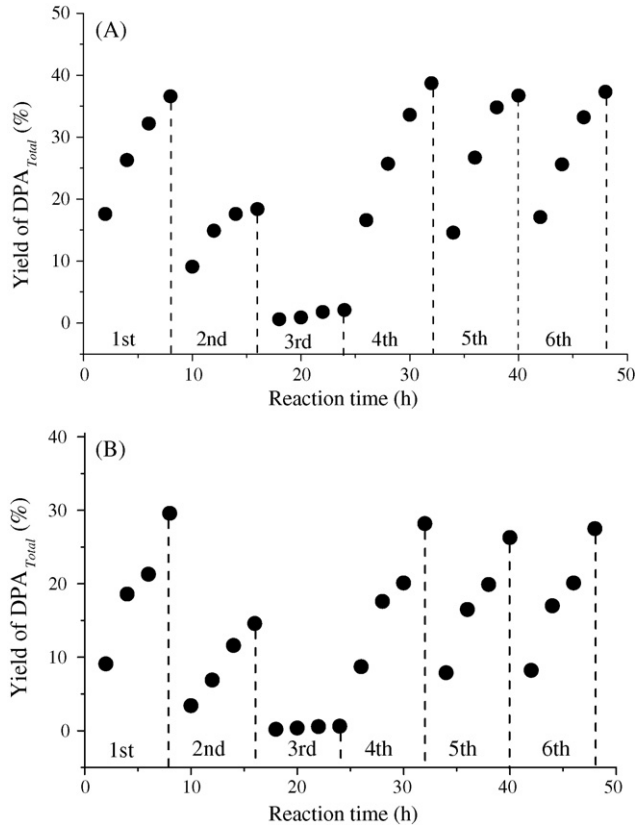

Fig. 9. Regeneration and deterioration of $H_3PW_{12}O_{40}/SiO_2$ materials for the synthesis of DPA from LA. (A) $H_3PW_{12}O_{40}/SiO_2$-E-14.8; (B) $H_3PW_{12}O_{40}/SiO_2$-C-15.7; 3.4 mmol LA; 13.6 mmol phenol; 50 mg catalyst; 100 °C. Temperature of regeneration of the catalyst was 120 °C (the second and third run) and 420 °C (fourth, fifth, and sixth run), respectively.

is enhanced by larger surface area and larger pore volume [20]. However, if the $H_3PW_{12}O_{40}$ loading is too high, the BET surface area and pore volume are strongly reduced. Among 10 $H_3PW_{12}O_{40}/SiO_2$ materials studied, the catalytic activity for $H_3PW_{12}O_{40}/SiO_2$-C-15.7 and $H_3PW_{12}O_{40}/SiO_2$-E-17.5 are the highest, whereas $H_3PW_{12}O_{40}/SiO_2$-E-4.0 and $H_3PW_{12}O_{40}/SiO_2$-C-7.5 are the lowest. These results are consistent with the most active materials being those with the largest number of available active sites, larger pore diameter, and ordered mesostructure. For the $H_3PW_{12}O_{40}/SiO_2$-C-58.2 and $H_3PW_{12}O_{40}/SiO_2$-C-65.1 materials, the number of active sites available decreased due to the lower BET surface areas even though their $H_3PW_{12}O_{40}$ loadings are the highest. In addition, their mesostructure is poorly ordered, which significantly affects the accessibility and rate of diffusion for the reactants and the products [28]. Uneven dispersion of the Keggin units in the composites also results in decreased catalytic activity. The low activity of $H_3PW_{12}O_{40}/SiO_2$-15.4 without P123 is mainly due to its narrow pore diameter (1.2 nm) and disordered pore structure. For the condensation reaction of phenol with LA to produce DPA, the sizes of the products (*p,p'*-DPA and *o,p'*-DPA) are large. Therefore, the catalyst with the larger pore size is favorable for better accessibility of the acidic sites. Too narrow a pore size increases internal mass transfer resistance, resulting in less space being available within the pore for the incoming reactants. Additionally, calcination of the catalyst at 420 °C for surfactant removal may lose a few acid sites compared with extracted catalyst, which results in lower activity of $H_3PW_{12}O_{40}/SiO_2$-15-C-7.5 compared to $H_3PW_{12}O_{40}/SiO_2$-C-7.5.

Table 4
Synthesis of DPA from LA catalyzed by $H_3PW_{12}O_{40}/SiO_2$-E-17.5 at different reaction temperatures

Temperature (°C)	Yield (%)	*p,p'*:*o,p'* (molar ratio)
80	8.2	3.3
100	18.9	2.8
120	22.1	2.0

After the reaction, the catalyst was removed by hot filtration. The catalyst-free reaction liquor was returned to reaction conditions (100 °C, 8 h) and monitored further. No further conversion of LA was detected, consistent with a stable heterogeneous catalyst. Furthermore, analysis of the solution by ICP-AES shows that no significant amount of $H_3PW_{12}O_{40}$ leached into the reaction. The recovered catalysts were washed with hot water and EtOH, respectively, and then being calcined at 120 °C in a vacuum for 60 min for the second and third runs. However, the catalytic activity was partially lost by the second catalytic cycle and in the third run, almost all of the activity was lost (Fig. 9). However, leaching of $H_3PW_{12}O_{40}$ was still hardly detectable by ICP-AES, implying that the loss of the catalytic activity for $H_3PW_{12}O_{40}/SiO_2$ is due to the strong adsorption of DPA molecules on the $H_3PW_{12}O_{40}/SiO_2$ composite. Therefore, we calcined the reused catalysts at 420 °C for the 4–6th runs, and the catalytic activity was restored.

4. Conclusion

It is a challenge to prepare mesoporous HPA-silica composite catalyst with unique surface physicochemical properties and highly dispersed HPA. By precise design the homogeneous Keggin unit ($H_3PW_{12}O_{40}$) was successfully heterogenized on silica matrix *via* a direct sol–gel–hydrothermal method in the presence of a triblock copolymer surfactant (P123). The structural integrity of the Keggin unit remained intact after formation of the composite catalysts. The materials exhibit higher BET surface area, high porosity, larger and well-defined pore size, and evenly dispersed catalytic sites across the materials. The materials show excellent catalytic activity in the reaction of the important bio-platform molecule LA with phenol to produce DPA. The leaching of $H_3PW_{12}O_{40}$ is effectively avoided. By using a suitable catalyst regeneration method, the materials can be reused several times without loss of activity. This work demonstrates green and efficient heterogeneous acid catalysts for use in the reaction of a building block chemical obtained from biomass.

Acknowledgments

We thank to Professor Hong Ding, School of Chemistry, Jilin University, PR China, for providing LC–MS results to current

work. This work was supported by the Program of New Century Excellent Talents in University (NCET-04-0311), the Key Project of Chinese Ministry of Education (No. 308008), and the Analysis and Testing Foundation of Northeast Normal University.

References

[1] J.J. Bozell, L. Moens, D.C. Elliott, Y. Wang, G.G. Neuenscwander, S.W. Fitzpatrick, R.J. Bilski, J.L. Jarnefeld, Resour. Conserv. Recycl. 28 (2000) 227.
[2] Y. Isoda, M. Azuma, Japanese Patent 08053390, Honshu Chemical Ind., (1996).
[3] Q. Yang, J. Liu, J. Yang, M.P. Kapoor, S. Inagaki, C. Li, J. Catal. 228 (2004) 265.
[4] J.Y. Cha, M.A. Hanna, Ind. Crops Prod. 16 (2002) 109.
[5] A. Taguchi, F. Schüth, Microporous Mesoporous Mater. 77 (2005) 1.
[6] I.V. Kozhevnikov, J. Mol. Catal. A: Chem. 1/2 (2007) 86.
[7] M. Misono, Chem. Commun. 13 (2001) 1141.
[8] T. Okuhara, Chem. Rev. 102 (2002) 3641.
[9] Y. Izumi, M. Ono, M. Kitagawa, M. Yoshida, K. Urabe, Microporous Mater. 5 (1995) 255.
[10] Y. Guo, Y. Wang, C. Hu, E. Wang, Chem. Mater. 12 (2000) 3501.
[11] Y. Guo, C. Hu, C. Jiang, Y. Yang, S. Jiang, X. Li, E. Wang, J. Catal. 217 (2003) 141.
[12] Y. Guo, C. Hu, S. Jiang, C. Guo, Y. Yang, E. Wang, Appl. Catal. B: Environ. 36 (2002) 9.
[13] Y. Guo, D. Li, C. Hu, Y. Wang, E. Wang, Appl. Catal. B: Environ. 3/4 (2001) 337.
[14] I.V. Kozhevnikov, K.R. Kloetstra, A. Sinnema, H.W. Zandbergen, J. Mol. Catal. A: Chem. 114 (1996) 287.
[15] D.P. Sawant, A. Vinu, N.E. Jacob, F. Lefebvre, S.B. Halligudi, J. Catal. 235 (2005) 341.
[16] Y. Izumi, K. Hisano, T. Hida, Appl. Catal. A: Gen. 181 (1999) 277.
[17] Y. Guo, C. Hu, X. Wang, E. Wang, Y. Zhou, S. Feng, Chem. Mater. 13 (2001) 4058.
[18] M.J. Verhoef, P.J. Kooyman, J.A. Peters, H. van Bekkum, Microporous Mesoporous Mater. 27 (1999) 365.
[19] Q.H. Xia, K. Kidajat, S. Kawi, J. Catal. 209 (2002) 433.
[20] Z. Liu, E. Lindner, H.A. Mayer, Chem. Rev. 102 (2002) 3543.
[21] M.T. Pope, A. Müller, Angew. Chem. Int. Ed. Engl. 30 (1991) 34.
[22] D. Zhao, Q. Huo, J. Feng, B.F. Chmelka, G.D. Stucky, J. Am. Chem. Soc. 120 (1998) 6024.
[23] M. Kruk, M. Jaroniec, C.H. Ko, R. Ryoo, Chem. Mater. 12 (2000) 1961.
[24] L. Li, Q. Wu, Y. Guo, C. Hu, Microporous Mesoporous Mater. 87 (2005) 1.
[25] M. Misono, Chem. Commun. (2001) 1141.
[26] S. Jiang, Y. Guo, C. Wang, X. Qu, L. Li, J. Colloid Interface Sci. 208 (2007) 208.
[27] D. Margolese, J.A. Melero, S.C. Christiansen, B.F. Chmelka, G.D. Stucky, Chem. Mater. 12 (2000) 2448.
[28] J.H. Clark, D.J. Macquarrie, S.J. Tavener, Dalton Trans. (2006) 4297.